The behavior of these diamonds is typical of carrier-injection electroluminescence.[5] It is probable that electrons are injected into the conduction band at the point contact, the injection efficiency varying with position and frequency. These electrons then combine with holes in the valence band. The recombination must involve energy levels near the middle of the forbidden gap because the wavelengths corresponding to direct transitions would be shorter than 2500 A. The emission from interior points in one diamond probably indicated the presence of internal potential barriers.

It seems possible that the electroluminescence described is another characteristic of Type IIb diamonds in addition to the semiconducting properties, the phosphorescence, and the extra infrared absorption peaks.[2]

---

[5] G. Destriau and H. F. Ivey, Proc. Inst. Radio Engrs. **43**, 1911 (1955).

PHYSICAL REVIEW VOLUME 105, NUMBER 3 FEBRUARY 1, 1957

Elastic Scattering of Low-Energy Electrons by Atomic Nitrogen and Atomic Oxygen

Lawrence Baylor Robinson
The Ramo-Wooldridge Corporation, Los Angeles, California

(Received September 20, 1956)

The phase shifts and elastic scattering cross sections of atomic nitrogen and oxygen for low-energy electrons have been calculated with central field potentials. Most emphasis has been placed on the Hartree-Fock potentials. In the low-energy range, the WBKJ approximation gives an indefinitely increasing cross section, whereas the integration of the differential equation yields finite cross sections in the limit of zero energy, for both nitrogen and oxygen. The Hartree potential does not allow for the existence of a bound state (negative ion) in either case. The Thomas-Fermi potential, although not reliable for low atomic numbers, does allow for the existence of a bound state (of approximately zero energy) in the case of oxygen.

I. INTRODUCTION

An understanding of the various processes occurring in the upper atmosphere involves the scattering of low-energy electrons by atomic nitrogen and atomic oxygen. Experiments are difficult in the low-energy range because of the recombination of the atoms to form molecules. Two calculations of the low-energy elastic scattering cross section of atomic oxygen reported in the literature differ markedly.[1] They are shown in Fig. 1. The cross section given by Mitra, Ray, and Ghosh seems to increase without limit as the electron energy goes to zero (cross sections are given up to 1000 atomic units) whereas the largest value given by Yamanouchi for the limiting case of zero (incident electron) energy is only about 85 atomic units. One of the purposes of this article is to give some insight regarding the cause of this discrepancy.

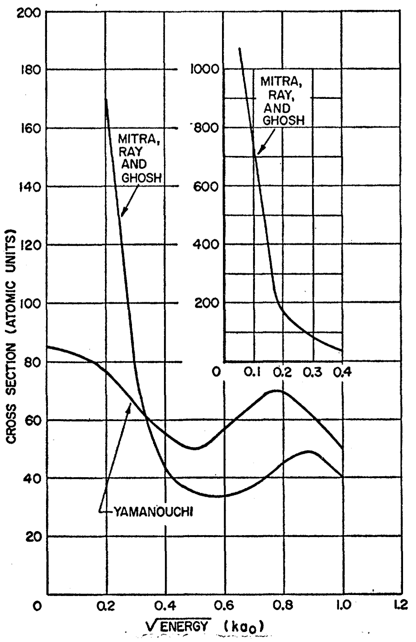

Fig. 1. Previously reported cross section for low-energy electrons and atomic oxygen.

It is well known that the method of Faxen and Holtzmark can give satisfactory results for elastic scattering from central field potentials. However, one does not know just how to modify the unperturbed *atomic* potentials in order to take into account exchange and polarization effects resulting from incoming electrons. More experimental information is needed to provide a basis for the selection of one out of several alternate methods of accounting for these perturbations. Maintaining a central field approximation has obvious advantages. Holtzmark[2] was able to obtain agreement between theory and experiment for argon and krypton by using a Hartree field modified by another simple central field to account for exchange and polarization effects. Experiments with rare gas atoms can be carried out more

---

[1] Mitra, Ray, and Ghosh, Nature **145**, 1017 (1940); T. Yamanouchi, Progr. Theoret. Phys. Japan **2**, 23 (1947).

[2] J. Holtzmark, Z. Physik **55**, 437 (1929); **66**, 49 (1930).

easily than with nitrogen and oxygen atoms because the rare gas atoms do not combine to form molecules.

The calculations reported in this article were made first with the unmodified Hartree-Fock fields. The sensitivity of the zero-energy cross sections to the form of the potential was demonstrated by the use of the Thomas-Fermi potential. Even though this potential is not reliable for atoms of low atomic number (Z), a significant phenomenon results from its use. These calculations were made by the Computer Systems Division (Ramo-Wooldridge) with the ERA Model 1103 Univac Scientific Digital Computer. Apart from these results, an additional program is under way to give more insight into the quantitative effect of various parts of the potential on scattering in general.

Some of the mathematical aspects will be discussed in detail so that the reader will be able to evaluate the range of validity and extent of applicability of the results. Mitra, Ray, and Ghosh do not indicate how their calculations were made. Yamanouchi integrated (numerically) the scattering differential equation.

II. MATHEMATICAL FORMULATION

Transport properties of electrons involve the momentum transfer (also called diffusion) cross section[3]:

$$Q_M=\frac{2\pi}{k^2}\int_0^{2\pi} \left|\sum_{l=0}^{\infty} (2l+1)e^{i\delta_l}\sin\delta_l P_l(\cos\theta)\right|^2(1-\cos\theta)\sin\theta d\theta$$

$$=Q_0-Q'=\frac{4\pi}{k^2}\left[\sum_{l=0}^{\infty}(2l+1)\sin^2\delta_l-\sum_{l=0}^{\infty}(2l+2)\cos(\delta_{l+1}-\delta_l)\sin\delta_{l+1}\sin\delta_l\right]. \tag{1}$$

One may write $Q_0=\sum_{l=0}^{\infty}\sigma_l$ where

$$\sigma_l=4\pi(2l+1)\sin^2\delta_l/k^2.$$

The phase shifts, δ_l, are obtained from the solution of the differential equation which governs the radial part of the Schrödinger wave function,

$$\frac{d^2y_l}{dr^2}+\left\{[E-V(r)]\frac{2m}{\hbar^2}+\frac{l(l+1)}{r^2}\right\}y_l=0. \tag{2}$$

The principal potential used in these calculations may be written as

$$V(x)=-\frac{\epsilon^2}{a_0x}\left[Z-\int_0^x \sum q_{nl}P_{nl}^2(t)dt -x\int_x^{\infty}\sum q_{nl}P_{nl}^2(t)\frac{dt}{t}\right]$$

$$=-Z(x)\epsilon^2/a_0x.\quad (x=r/a_0). \tag{3}$$

In Eq. (3), the q's refer to the number of electrons having a given wave function and the P's are the P_{1s}, P_{2s}, and P_{2p} Hartree-Fock one-electron wave functions for the $1s$, $2s$, and $2p$ electrons in nitrogen[4] and oxygen[5] atoms. The electron densities are shown in Fig. 2. The functions corresponding only to the ground states, ^4S and ^3P, respectively, are considered at this time.

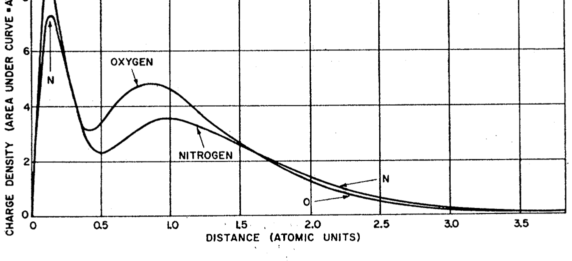

FIG. 2. Hartree electron densities.

Approximate phase shifts can be obtained by the WBKJ solutions of Eq. (2). The phase shifts are given, in this approximation, by[6]

$$\delta_l=\int_{x_2}^{\infty}\left[(ka_0)^2-\frac{2mV(x)a_0^2}{\hbar^2}-\frac{(l+\frac{1}{2})^2}{x^2}\right]^{\frac{1}{2}}dx -\int_{x_1}^{\infty}\left[(ka_0)^2-\frac{(l+\frac{1}{2})^2}{x^2}\right]^{\frac{1}{2}}dx. \tag{4}$$

This approximation is assumed valid for the cases in which the potential does not change much over one wavelength of the incoming electron.

More exact phase shifts are obtained by the numerical integration of Eq. (2). An abbreviated version of the manner in which the Computer System Division carried through the numerical integrations in order to obtain the phase shifts follows.

Equation (2) may be written more compactly as

$$y''+\left[(\lambda+AV(x))-\frac{l(l+1)}{x^2}\right]y=0, \tag{5}$$

---

[3] H. S. W. Massey and E. H. S. Burhop, *Electronic and Ionic Impact Phenomena* (Oxford University Press, New York, 1952), p. 15. Dr. H. Einbinder suggested the final form of Eq. (1).

[4] D. R. Hartree and W. H. Hartree, Proc. Roy. Soc. (London) **A193**, 299 (1948).

[5] Hartree, Hartree, and Swirles, Trans. Roy. Soc. **A238**, 229 (1939).

[6] E.g., P. M. Morse and H. Feshbach, *Methods of Theoretical Physics* (McGraw-Hill Book Company, Inc., New York, 1953), Part II, pp. 1101–1103.

TABLE I. WKBJ phase shifts and cross sections (in units of a_0^2) for electron-nitrogen scattering.

ka_0	l	δ_l	σ_l (a_0^2)	Q_0 (a_0^2)
0.25	0	5.01	185	185
0.50	0	4.73	50.2	
	1	0.025	···	50.2
0.75	0	4.46	21.0	
	1	1.48	66.5	87.5
1.00	0	4.23	9.75	
	1	1.67	37.2	
	2	0.036	0.078	47.0
1.50	0	3.84	2.34	
	1	1.72	16.4	
	2	0.188	0.974	
	3	0.033	···	19.7

TABLE II. WKBJ phase shifts and cross sections (in units of a_0^2) for electron-oxygen scattering.

ka_0	l	δ_l	σ_l (a_0^2)	Q_0 (a_0^2)
0.25	0	5.14	167	167
0.50	0	4.89	58.6	
	1	0.014	···	48.6
0.75	0	4.64	22.3	
	1	1.45	66.0	88.3
1.00	0	4.42	11.6	
	1	1.72	36.8	
	2	0.022	···	48.4
1.50	0	4.05	3.48	
	1	1.82	15.8	
	2	0.130	0.47	
	3	0.021	···	19.8

where $\lambda=(ka_0)^2$ and $A=2ma_0^2/\hbar^2$. A solution $[y(0)=0]$ is obtained within the region where $V(x)\neq 0$. This solution is connected with the asymptotic solution which is obtained beginning with the point where $V(x)=0$. A comparison of this solution with the one obtained for $V(x)=0$ everywhere, provides the phase shifts from which the cross sections are calculated.

The potential has the following approximate form, near the origin:

$$V(x)=(b_0/x)+b_1+b_2x. \tag{6}$$

Equation (5) then becomes

$$x^2y''+[\lambda x^2+A(b_0x+b_1x^2+b_2x^3)-l(l+1)]y=0. \tag{7}$$

A form of solution by the method of Frobenius,

$$y=x^\alpha\sum_{n=0}^{\infty}C_nx^n,\quad C_0=1 \tag{8}$$

when substituted in (8) yields the following indicial equation:

$$\alpha(\alpha-1)C_0-l(l+1)C_0=0,\quad \alpha=l+1,\quad \alpha=-l. \tag{9}$$

Since $y(0)=0$, only $\alpha=l+1$ is acceptable. The recursion formula for the coefficients is

$$C_n=\frac{-[Ab_0C_{n-1}+(\lambda+Ab_1)C_{n-2}+Ab_2C_{n-3}]}{(\alpha+n)[\alpha+(n-1)]-l(l+1)}. \tag{10}$$

Both the function y and the derivative y' were determined at $x=0.1$ and then a modified Runge-Kutte technique was used to continue the solution out to the point where the potential vanishes.

If the point at which the potential vanishes is called $\bar{x}$, then for $x\geq\bar{x}$, Eq. (5) becomes

$$y''+\left[\lambda-\frac{l(l+1)}{x^2}\right]y=0, \tag{11}$$

and the following form is taken for the solution:

$$y=\exp[i(\lambda^{\frac{1}{2}}x)]\left(1+\frac{a_1}{x}+\frac{a_2}{x^2}+\cdots\right). \tag{12}$$

When this is substituted in Eq. (11), the recursion formula

$$a_n=\frac{a_{n-1}[n(n-1)-l(l+1)]}{2ni\lambda^{\frac{1}{2}}}, \tag{13}$$

is obtained. The general solution of the equation is

$$y_l=D_1\,\mathrm{Re}(y)+D_2\,\mathrm{Im}(y), \tag{14}$$

where

$$\begin{aligned}\mathrm{Re}(y)&=\cos[(\lambda^{\frac{1}{2}}x)]\left[1+\frac{l(l+1)(2-l^2-l)}{8\lambda x^2}+\cdots\right]\\&\quad+\sin[(\lambda^{\frac{1}{2}}x)]\left[-\frac{l(l+1)}{2\lambda^{\frac{1}{2}}x}+\cdots\right],\\\mathrm{Im}(y)&=\sin[(\lambda^{\frac{1}{2}}x)]\left[1+\frac{l(l+1)(2-l^2-l)}{8\lambda x^2}+\cdots\right]\\&\quad+\cos[(\lambda^{\frac{1}{2}}x)]\left[-\frac{l(l+1)}{2\lambda^{\frac{1}{2}}x}+\cdots\right].\end{aligned} \tag{15}$$

The coefficients D_1 and D_2 in Eq. (14) will determine the phase shifts in the fashion shown immediately below. If one writes the numerical solutions up to the point $\bar{x}$ as $Y_l(x)$, then at $\bar{x}$

$$\begin{aligned}Y_l(\bar{x})&=D_1\ \mathrm{Re}[y(\bar{x})]+D_2\ \mathrm{Im}[y(\bar{x})],\\Y_l'(\bar{x})&=D_1\,\mathrm{Re}'[y(\bar{x})]+D_2\,\mathrm{Im}'[y(\bar{x})].\end{aligned} \tag{16}$$

These two equations in two unknowns provide D_1 and D_2. The asymptotic solution (i.e., for large x) is

$$\begin{aligned}y_l&=D_1\cos(\lambda^{\frac{1}{2}}x)+D_2\sin[(\lambda^{\frac{1}{2}}x)]\\&=(D_1^2+D_2^2)^{\frac{1}{2}}\sin[(\lambda^{\frac{1}{2}}x)+\phi],\end{aligned} \tag{17}$$

where

$$\tan\phi = D_1/D_2,\qquad \delta_l = \phi + \tfrac{1}{2}\pi l. \tag{18}$$

The phase shifts were determined by both Eqs. (4) and (18).

The limiting cross section for zero electron energy is obtained as given below.[7] As the energy approaches zero, only the $l=0$ phase shift is different from zero. From Eq. (1),

$$Q_M = (4\pi/k^2)\sin^2\delta_0. \tag{19}$$

Equation (5) becomes

$$y'' + AV(x)y = 0. \tag{20}$$

Outside $\bar{x}$, the solution starts out like a straight line

$$y = Cx + \beta, \tag{21}$$

where C is the slope and β is the intercept on the y axis. The asymptotic form, Eq. (17), can be approximated by Eq. (21) if one writes $y \sim B(\lambda^{\frac{1}{2}}x + \delta_0)$. Hence δ_0, the y intercept, is given by $\delta_0 = -\lambda^{\frac{1}{2}}x_0$. When this is substituted in Eq. (19) with the approximation that $\sin^2\delta_0 \sim \delta_0^2$, then

$$\sigma_0 = 4\pi x_0^2, \tag{22}$$

where $x_0 = -\beta/C$ [from Eq. (21)]. The Thomas-Fermi potential was also used in Eq. (22).

The signs of the slope, x intercept and y intercept give information regarding the possibility of the existence of a bound state (i.e., negative ion) with about zero binding energy. The extrapolated wave function must have a negative slope and must cross the x axis at some positive x_0 for such a state to exist. On the other hand, a positive slope and positive x intercept mean that such a bound state cannot exist. The other possibilities imply that a bound state can "almost" exist. The situation is summarized in the following equation.

$$\begin{array}{lll} \beta<0, & C>0, \quad x_0>0: & \text{no bound state can exist;} \\ \beta\geq 0, & C\geq 0, \quad 0\geq x_0\geq -\infty: & \text{a bound state "almost" exists (especially if } C\sim 0\text{);} \\ \beta>0, & C<0, \quad x_0>0: & \text{a bound state can exist with about zero binding energy.} \end{array} \tag{23}$$

III. RESULTS

The phase shifts and cross sections as calculated in the WBJK approximation are given in Tables I and II, respectively, for nitrogen and oxygen. For lower energies ($ka_0 \approx 0.13$) multiple zeros appear, and even though procedures for selecting the proper zero have been discussed, interpretations are not unambiguous.[8] The cross

TABLE III. Differential equation phase shifts and cross sections for electron-nitrogen scattering.

ka_0	l	δ_l	σ_l (πa_0^2)	Q_0 (a_0^2)	Q_M (a_0^2)
0.0032	0	6.27	46.1	145	145
0.0710	0	6.04	44.6	140	140
0.100	0	5.95	43.1	136	136
0.141	0	5.81	40.4	127	127
0.200	0	5.64	35.8		
	1	0.0151	0.1	113	113
0.284	0	5.41	29.0		
	1	0.044	0.3	92.0	92.0
0.448	0	5.05	17.8		
	1	0.197	2.3	63.1	63.1
0.710	0	4.62	7.9		
	1	0.878	14.2	69.5	37.1
1.00	0	4.28	3.3		
	1	1.51	12.0	48.0	26.3
1.41	0	3.92	1.0		
	1	1.68	5.9		
	2	6.46	0.3	22.7	16.8
2.24	0	3.39	···		
	1	1.61	2.4		
	2	6.73	0.8		
	3	6.41	···	9.9	9.6

TABLE IV. Differential equation phase shifts and cross sections for electron-oxygen scattering.

ka_0	l	δ_l	σ_l (πa_0^2)	Q_0 (a_0^2)	Q_M (a_0^2)
0.0032	0	6.27	27.0	84.8	84.8
0.0710	0	6.10	26.5	83.3	83.3
0.100	0	6.02	26.0	81.6	81.6
0.141	0	5.92	25.0	78.5	78.5
0.200	0	5.78	23.3		
	1	0.0124	···	73.3	73.3
0.284	0	5.59	20.4		
	1	0.0364	0.2	64.7	64.7
0.448	0	5.26	14.6		
	1	0.164	1.6	50.8	50.8
0.710	0	4.75	7.8		
	1	0.813	12.7	64.0	41.0
1.00	0	4.50	3.8		
	1	1.57	12.0	49.6	25.4
1.41	0	4.14	1.4		
	1	1.79	5.7		
	2	6.41	0.2	23.0	15.9
2.24	0	3.61	0.2		
	1	1.72	2.3		
	2	6.37	0.6		
	3	6.30	···	9.7	7.7

---

[7] E.g., Fermi, Orear, Rosenfeld, and Schluter, *Nuclear Physics* (University of Chicago Press, Chicago, 1950), revised edition, p. 119; J. Schwinger, *Nuclear Physics* (Reproduced at Boston University, Boston, 1955), Part II, pp. 54–56.

[8] N. F. Mott and H. S. W. Massey, *The Theory of Atomic Collisions* (Oxford University Press, London, 1949), second edition, pp. 127–128.

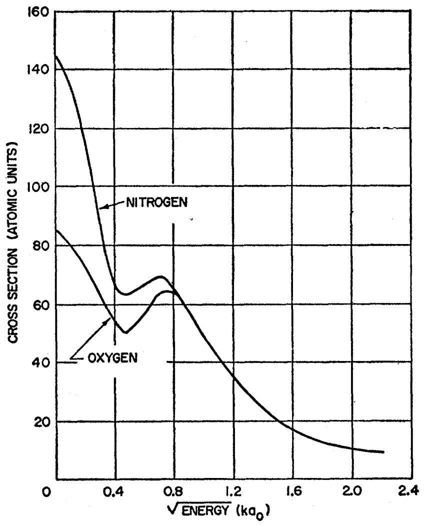

FIG. 3. Elastic scattering cross sections for electrons and atomic oxygen and atomic nitrogen.

sections seem to increase indefinitely. The shape of the curve reported by Mitra, Ray, and Ghosh for atomic oxygen is reproduced in the WBKJ approximation. Evidently this is the manner in which they calculated the oxygen cross section. In the present calculation, only the unmodified Hartree potential was used.

Tables III and IV show the phase shifts and cross sections which were obtained from the integration of the differential equations with the Hartree potential. These cross sections go to a finite number in the limit of zero energy. The limit for oxygen is the same as that given by Yamanouchi, and the calculation reproduces his curve. The S-phase shifts approach the number 2π as the electron energy goes to zero. In the energy range less than about 0.5 ev, the scattering and momentum transfer cross sections are identical. For higher energies, it can be a poor approximation to assume that the cross sections are identical because of the strong angular dependence.

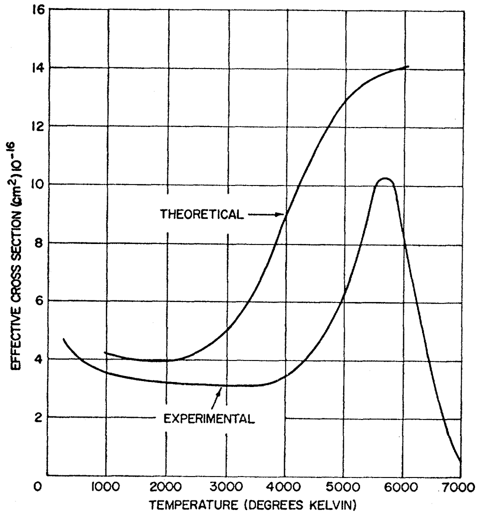

FIG. 4. Experimental and theoretical cross sections for scattering of electrons with air.

Figure 3 shows the information contained in Tables III and IV in graphical form. Beyond 9 ev the cross sections are practically indistinguishable and only one line has been drawn to represent both oxygen and nitrogen. These electrons have sufficient energy to penetrate to such a depth that scattering occurs essentially by the $1s^2$ electrons. As can be seen from Fig. 2, the density distributions are not too different. The outer electronic distribution extends farther for nitrogen and is somewhat larger than for oxygen. The low-energy electrons are scattered essentially by these electrons; evidently this accounts for a larger nitrogen cross section than for oxygen.

Table V gives the parameters (Eqs. 21 and 22) for the limiting case of zero energy. A reference to Eq. (23) will show that the Hartree potential does not allow for a bound state of either nitrogen or oxygen.

Evidence from mass spectrograph studies[9] shows the existence of a stable negative ion of oxygen (O^-) and the nonexistence of N^-. Bates[10] studied the following two configurations for O^-, $1s^22s^22p^5$, and $1s^22s^22p^43s$ and concluded that the $2p^43s$ should be about 2 ev higher than the $2p^5$. Since the electron affinity of oxygen is about 1.5–2 ev, the excited state ($3s$) of O^- should be able to exist with about zero binding energy. The scattering potential which the electron sees should reflect this. Since the Hartree potential does not allow for the bound state, the Thomas-Fermi potential was examined. The results (Table V) show that this potential is able almost to induce a bound state in the nitrogen atom and is able to bind an electron with about zero energy in the oxygen atom. This potential also gives a larger cross section for oxygen then for nitrogen. Evidently a more reasonable scattering potential lies somewhere between the Hartree and Thomas-Fermi potentials. Accurate experimental information is needed to decide how to modify the potentials with the proper polarization correction.

TABLE V. Parameters for cross section at zero energy [Eqs. (21) and (22)].

Atom	C	β	x_0 (a_0)	Q (a_0^2)
		Hartree-Fock field		
Nitrogen	0.0604	−0.205	3.40	145
Oxygen	0.0710	−0.185	2.60	84.9
		Thomas-Fermi field		
Nitrogen	0.0165	0.824	−23.2	6700
Oxygen	−0.00533	0.987	80.9	82 000

---

[9] R. H. Sloane and H. M. Love, Nature **159**, 302 (1947).
[10] D. R. Bates, Proc. Roy. Irish Acad. **A51**, 151 (1947).

The cross sections given in Fig. 3 were used in conjunction with cross sections calculated for the molecular species (by Fisk[11]) as a basis for some comparison with experiment. Maecker[12] examined some experiments on free-burning arcs and, assuming equilibrium prevailing at atmospheric pressure, obtained the "effective" (*wirkungs*) cross section of air for electron collisions as a function of temperature. Figure 4 shows this mean (*gemittelte*) curve compared with results obtained as explained immediately above. The shape of the Maecker's curve is partially reproduced. One of his curves fits this calculation better, but there was no basis for selecting anything other than his mean curve. Beyond 6000°K, the calculated cross section does not decrease as the experimental curve indicates. The cross sections for the atomic species cannot be compared with the experiment in this case in the very low-energy range. This is because of the small amounts of dissociation at low temperatures. Perhaps the theoretical wave should be averaged over some velocity distribution of neutral particles.

The composition of air was obtained from a Lockheed Aircraft Corporation report.[13] Table VI gives the values taken from Fisk's graphs; Table VII gives the composition of air as a function of temperature at atmospheric pressure, as well as the contribution of each species to the cross section.

TABLE VI. Fisk's cross sections for (molecular) nitrogen and oxygen.

ka_0	T(1000°K)	$\sqrt{V}$ (electron volts)$^{\frac{1}{2}}$	Cross section (a_0^2) Nitrogen	Oxygen
0.098	1.0	0.36	16	12
0.14	2.0	0.51	16	12
0.17	3.0	0.62	18	11
0.20	4.0	0.72	20	12
0.22	5.0	0.80	21	12
0.24	6.0	0.87	23	13
0.26	7.0	0.95	24	13

TABLE VII. Composition of air as a function of temperature at atmospheric pressure, and the contribution of each species to the cross section.

T(1000°K) / $\log(\rho/\rho_0)$ / Constituent	1 −0.562	2 −0.865	3 −1.039	4 −1.170	5 −1.260	6 −1.340
Mole fractions of various constituents						
N_2	0.780	0.777	0.743	0.663	0.621	0.509
O_2	0.209	0.205	0.162	0.0417	0.00338	...
N	...	...	...	0.00150	0.0279	0.163
O	...	...	0.0427	0.249	0.318	0.308
Cross section Q_0 (in units of a_0^2)						
N_2	13	12	13	13	13	12
O_2	2	2	2	0.5	0.04	...
N	...	...	...	...	3	18
O	...	...	3	18	21	19
Total Q_0 (a_0^2)	15	14	18	32	47	49
Total Q_0 (10^{-16} cm^2)	4.2	3.9	5.0	9.0	13	14

Evidently the cause of the discrepancy in the work of Yamanouchi and that of Mitra *et al.* has been found. Yamanouchi's calculations for atomic oxygen are in good agreement with those reported here.

The next part of this study will involve the effects of polarization potentials on the cross section. In addition, for oxygen, a potential will be used in which the electron density is determined from Slater wave functions which give a more realistic value of the electron affinity than that given by the Hartree-Fock functions.

The writer has profited from stimulating discussions with Dr. S. Altshuler, Dr. H. Einbinder, and Dr. H. E. Wohlwill during the preparation of this article. Appreciation is expressed to the Ramo-Wooldridge Computer Systems Division; personal contact has been made with Dr. David Young, Jr., Mr. Werner Frank, Mr. Horace Flatt, Mr. T. L. Emrick, and especially Mr. Frank Meek.

---

[11] J. B. Fisk, Phys. Rev. **49**, 167 (1936).

[12] H. Maecker, Z. Physik **128**, 289 (1950).

[13] J. W. Bond and J. N. Dyer, Lockheed Aircraft Corporation Report No. MSD 1487, December 30, 1955 (unpublished).